

RESEARCH

Open Access



Engineering a PhrC-RapC-SinR quorum sensing molecular switch for dynamic fine-tuning of menaquinone-7 synthesis in *Bacillus subtilis*

Xuli Gao¹, Yani Luo¹, Elvis Kwame Adinkra¹, Yu Chen^{1,2}, Wei Tao¹, Yongyuan Liu¹, Mingyu Guo¹, Jing Wu¹, Chuanchao Wu^{1,2,3} and Yan Liu^{1,2,3*}

Abstract

Background Menaquinone-7 (MK-7) is a valuable vitamin K₂ produced by *Bacillus subtilis*. Although many strategies have been adopted to increase the yield of MK-7 in *B. subtilis*, the effectiveness of these common approaches is not high because long metabolic synthesis pathways and numerous bypass pathways competing for precursors with MK-7 synthesis. Regarding the modification of bypass pathways, studies of common static metabolic engineering method such as knocking out genes involved in side pathway have been reported previously. Since byproducts phenylalanine (Phe), tyrosine (Tyr), tryptophan (Trp), folic acid, dihydroxybenzoate, hydroxybutanone in the MK-7 synthesis pathway are indispensable for cell growth, the complete knockout of the bypass pathway restricts cell growth, resulting in limited increase in MK-7 synthesis. Dynamic regulation via quorum sensing (QS) provides a cost-effective strategy to harmonize cell growth and product synthesis, eliminating the need for pricey inducers. SinR, a transcriptional repressor, is crucial in suppressing biofilm formation, a process closely intertwined with MK-7 biosynthesis. Given this link, we targeted SinR to construct a dynamic regulatory system, aiming to modulate MK-7 production by leveraging SinR's regulatory influence.

Results A modular PhrC-RapC-SinR QS system is developed to dynamic regulate side pathway of MK-7. In this study, first, we analyzed the SinR-based gene expression regulation system in *B. subtilis* 168 (BS168). We constructed a promoter library of different abilities, selected suitable promoters from the library, and performed mutation screening on the selected promoters. Furthermore, we constructed a PhrC-RapC-SinR QS system to dynamically control the synthesis of Phe, Tyr, Trp, folic acid, dihydroxybenzoate, hydroxybutanone in MK-7 synthesis in BS168. Cell growth and efficient synthesis of the MK-7 production can be dynamically balanced by this QS system. Using this system to balance cell growth and product fermentation, the MK-7 yield was ultimately increased by 6.27-fold, from 13.95 mg/L to 87.52 mg/L.

[†]Yani Luo: the same contribution to the paper.

*Correspondence:

Yan Liu
liuyan@ahpu.edu.cn

Full list of author information is available at the end of the article

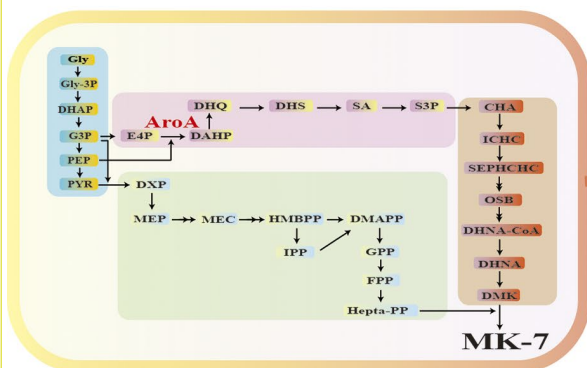


© The Author(s) 2025. **Open Access** This article is licensed under a Creative Commons Attribution-NonCommercial-NoDerivatives 4.0 International License, which permits any non-commercial use, sharing, distribution and reproduction in any medium or format, as long as you give appropriate credit to the original author(s) and the source, provide a link to the Creative Commons licence, and indicate if you modified the licensed material. You do not have permission under this licence to share adapted material derived from this article or parts of it. The images or other third party material in this article are included in the article's Creative Commons licence, unless indicated otherwise in a credit line to the material. If material is not included in the article's Creative Commons licence and your intended use is not permitted by statutory regulation or exceeds the permitted use, you will need to obtain permission directly from the copyright holder. To view a copy of this licence, visit <http://creativecommons.org/licenses/by-nc-nd/4.0/>.

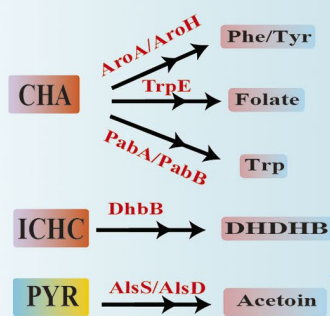
Conclusion In summary, the PhrC-RapC-SinR QS system has been successfully integrated with biocatalytic functions to achieve dynamic metabolic pathway control in BS168, which has potential applicability to a large number of microorganisms to fine-tune gene expression and enhance the production of metabolites.

Graphical Abstract

MK-7 Synthesis

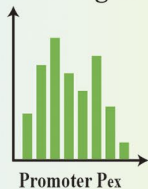


MK-7 Byproduct Pathway



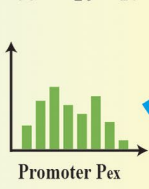
PepsA

binding site



-35 -16 -10

binding site



Promoter mutation



RapC → SinR → Pex

PhrC → RapC → SinR

P_{e11} P_{e9} P_{e9} P_{e9} P_{e16}
 aroA aroH trpE dhbB alsS-D
 target genes

Dynamic Fine-Tuning of MK-7 Synthesis

Keywords MK-7, SinR, PhrC-RapC, *Bacillus subtilis*

Introduction

Menaquinone-7 (MK-7), one of the three forms of vitamin K alongside phyloquinone (vitamin K1) and menadione (vitamin K3), distinguishes itself with remarkable bioavailability and an extended half-life. Emerging research has elucidated its multifaceted health benefits, encompassing the prevention of cardiovascular disease and osteoporosis, while also highlighting its promising therapeutic potential in the context of cancer, Alzheimer's disease, and Parkinson's disease. These attributes position MK-7 as a subject of considerable interest in both preventive healthcare and innovative therapeutic

strategies [1, 2]. The global aging population has led to a persistent annual increase in the incidence of age-related diseases such as cardiovascular disease, osteoporosis, cancer, Alzheimer's disease, and Parkinson's disease. This demographic shift poses a pressing and daunting challenge to healthcare systems worldwide, demanding effective strategies to manage these conditions. Current research underscores the absence of definitive curative treatments for these chronic ailments, thereby shifting the focus toward preventive approaches to mitigate their occurrence. In this context, the preventive potential of MK-7 has garnered significant attention, making

it a pivotal area of investigation [3, 4]. Consequently, the market for menaquinones, particularly MK-7, is substantial, driving considerable academic and industrial interest in its biosynthesis.

Bacillus subtilis 168 (BS168) is a preferred microbial strain for the production of MK-7, owing to several distinct advantages. First, *B. subtilis* has been granted Generally Recognized as Safe (GRAS) status by the U.S. Food and Drug Administration (FDA), attesting to its safety for applications in food, feed, and pharmaceuticals [5, 6]. Second, it serves as a promising bacterial chassis for secondary metabolite biosynthesis [7, 8]. BS168, in particular, is well-suited for modular metabolic engineering endeavor [9]. Additionally, the MK-7 biosynthetic pathway within BS168 has been clearly elucidated, facilitating targeted manipulations to enhance productivity [6, 10, 11]. These attributes collectively underscore the significance of BS168 as a superior host for MK-7 production, offering a versatile and efficient platform for biotechnological exploitation.

Researchers have explored various strategies to improve industrial-scale MK-7 production and biosynthetic efficiency. Due to the lengthy MK-7 synthetic pathway, modifying bypass pathways holds critical significance for enhancing MK-7 production. For instance, Yang utilized gene editing technology to knock out the two genes, *mgsA* and *araM*. This manipulation disrupted the conversion pathways of DHAP (dihydroxyacetone phosphate), a product in the glycerol dissimilation pathway, into MG (methylglyoxal) and G1P (glyceraldehyde 1-phosphate), thereby directing more DHAP towards the synthetic pathway of MK-7. Ultimately, this led to a 15% increase in MK-7 production [12]. Deletion of *dhbB* reduced the consumption of the intermediate metabolite isochorismate, thus promoting the yield of MK-7 to 15.4 ± 0.6 mg/L [9]. However, the complete knockout of these bypass genes has a significant impact on microbial growth. For instance, after knocking out the *mgsA* and *araM* genes, a notable decrease in microbial density was observed [12]. Additionally, the deletion of genes *dhbB* and *alsS-alsD* operon which are involved in by-product metabolic pathways, resulted in a dramatic decrease in the cell growth [9].

Dynamic regulatory systems have demonstrated their effectiveness in improving production by balancing cellular growth and metabolite synthesis [13]. Among these, quorum sensing (QS) systems, a form of dynamic regulation prevalent in bacteria, offer a cost-effective and non-toxic approach by eliminating the need for external inducers. QS enables bacteria to autonomously sense population density and trigger specific gene expression upon reaching a threshold, thereby dynamically modulating cellular behavior [14, 15]. The advent of synthetic biology has facilitated the harnessing of QS systems to

construct gene circuits that auto-regulate expression in response to bacterial growth, minimizing metabolic burden and enhancing target product yields [15–17]. For instance, Yang et al. engineered a QS circuit leveraging the cytokinin system and Ypd1-Skn7 pathway to dynamically degrade Erg9, achieving an 80% increase in α -farnesene production [18].

The Phr-Rap QS system in *Bacillus* comprises the response regulator aspartyl phosphate phosphatase (Rap) and its cognate inhibitory oligopeptide (Phr), which collectively orchestrate intricate signal transduction cascades in response to environmental cues [19]. As cell density increases, the extracellular concentration of Phr rises proportionally. Upon surpassing a critical threshold, Phr is actively transported into the cell via the oligopeptide permease (Opp), an ATP-dependent ABC transporter, where it binds to its cognate Rap protein, thereby attenuating its regulatory activity [20, 21]. Given the extensive characterization of the Phr-Rap QS system in *Bacillus*, it has emerged as a versatile tool for dynamically regulating metabolic pathways and biosynthesis [22–24]. For example, Hu harnessed the PhrQ-RapQ-DegU cascade to enhance gamma-polyglutamic acid (γ -PGA) production by 6.53-fold, underscoring the potential of QS-based strategies for metabolic engineering [25].

SinR, as a constitutively expressed transcriptional regulator that could regulate biofilm morphology in BS168 [26], was used to construct regulatory factor in Phr-Rap QS system for three reasons. Firstly, SinR could respond to Phr-Rap QS system. Previous studies found that SinR was controlled by ComA [27]. While ComA was regulated by RapC [22, 28], and PhrC stimulates ComA-dependent gene expression by repressing RapC [19, 28]. Secondly, SinR could affect the MK-7 synthesis. In our previously study, we construct a SinR mutant, which could form wrinkly and smooth biofilm morphology and enhance the MK-7 production to ten times [29]. We preliminarily determined the mechanism was that SinR mutant could regulate biofilm morphology [26, 30], a more wrinkly and smoother biofilm formed a network of interconnected channels with a low resistance to liquid flow and facilitate nutrient flow through the biofilm [31], finally affect MK-7 synthesis. In addition, the electrical hyperpolarization stimulated the synthesis of the electron transport chain components, such as cytochrome C and MK-7 [29]. Thirdly, SinR was a DNA-binding protein and binds to a consensus DNA binding sequence (5'-GTTCTYT-3', with Y representing an unspecified pyrimidine base) to repress DNA transcription [26, 30].

To address the challenge of enhancing MK-7 production in *Bacillus subtilis* while minimizing byproduct synthesis, we engineered a PhrC-RapC-SinR QS Molecular Switch. This switch was designed to dynamically repress the expression of bypass pathways by replacing

the native promoters of key enzymatic genes within the byproduct synthesis pathway with SinR-targeted promoters. By implementing this strategy, we aimed to modulate byproduct formation and redirect metabolic fluxes toward MK-7 production, all while maintaining optimal bacterial growth rates. The deployment of this system not only significantly elevates industrial MK-7 biosynthesis in *Bacillus subtilis* but also establishes a novel paradigm for improving secondary metabolite yields through quorum sensing-guided metabolic re-engineering.

Materials and methods

Strains and media

Table 1 lists the modified *B. subtilis* strains and corresponding plasmids used in this study; Table S1 provides primer sequences. All recombinant *B. subtilis* strains were derived from the laboratory stock strain *B. subtilis* 168. Strains were cultivated in Luria-Bertani (LB) medium or on LB agar plates at 37 °C for genetic experiments. The fermentation medium comprised 50 g/L soybean peptone, 50 g/L glycerol, 20 g/L yeast extract, 1.62 g/L KH_2PO_4 , and 3.86 g/L K_2HPO_4 . Antibiotics were added as follows: 50 µg/mL kanamycin (kan) and 10 µg/mL chloramphenicol (C_m^r).

DNA manipulation techniques

Bacillus subtilis 168 transformation was conducted using chemically competent cells prepared according to the calcium chloride method described by Liu et al. [25]. Genomic DNA extraction was performed using the TIANamp Bacteria DNA Kit, while plasmid purification and target fragment amplification were carried out with the TIANprep Mini Plasmid Kit and high-fidelity DNA Polymerase, respectively. Mutagenic DNA fragments were generated through overlap extension PCR (OE-PCR), wherein complementary terminal sequences were introduced to adjacent fragments. These fragments were subsequently ligated via homologous recombination in vivo following transformation into competent cells.

Construction of mutant strain

The upstream region of the *aroA* gene from BS168 (*L-aroA*), the chloramphenicol resistance gene ($-C_m^r$) from plasmid P7C6, and a fragment of the *aroA* gene from BS168 were individually cloned using primers (BS01-1 to BS01-6) as outlined in Table S1. Following successful cloning, each fragment was purified and subsequently fused to generate a contiguous *L-aroA-Cmr-aroA* construct. This construct was seamlessly integrated into the BS168 genome via chromosomal recombination, resulting in the mutant strain BS01. The same methodology was employed to construct other mutant strains.

Screening and mutation of promoter

To pinpoint promoters under SinR regulation, we first replaced the native *sinR* promoter with the inducible P_{grac100} promoter in strain BX00, allowing for precise control over SinR expression levels [32]. Next, we inserted eGFP downstream of target promoters using primers BX01–BX09 (Table S1), generating strains BX01–BX09. The fluorescence intensity emitted by eGFP served as a direct readout for promoter transcriptional efficiency. Once suitable promoters were identified, we engineered promoter mutants using primers P_{e1} – P_{e19} (Table S1). Specifically, we fused the chloramphenicol resistance gene ($-C_m^r$) with the mutants promoter fragment and replaced the suitable promoter, yielding strains BG1–BG19. Finally, we evaluated promoter activity in these engineered strains by quantifying their relative fluorescence intensity.

Fluorescence assay

Recombinant strains were inoculated into LB medium and cultivated at 37°C with shaking at 220 rpm for 12 h. Prior to fluorescence detection, strains were washed twice with PBS to remove any residual medium. The relative fluorescence intensity, calculated as the ratio of fluorescence intensity to optical density, was used as a measure of relative promoter transcription intensity. Both fluorescence intensity (at 490 nm) and optical density (at 600 nm) were measured using a microplate reader to ensure accurate quantification [25].

Construction of the PhrC-RapC-SinR regulatory system

To investigate the effects of RapC and the PhC-RapC on SinR, eGFP was inserted downstream of *sinR* using primers BP00-1 to BP00-6 (Table S1), resulting in strain BP00. Next, the P_{rapC} and P_{phrC} promoters in BP00 were replaced with P_{grac100} using primers BP01 and BP02 (Table S1), generating strains BP01 (BS168::*sinR*-eGFP:: P_{grac100} -*rapC*) and BP02 (BS168::*sinR*-eGFP:: P_{grac100} -*phrC*). This allowed for the regulation of RapC and PhrC expression by the inducer Isopropyl β-D-1-thiogalactopyranoside (IPTG). The changes in fluorescence intensity within BP01 and BP02 bacterial cultures were monitored to examine the regulatory relationships between PhC, RapC, and SinR.

To construct the PhrC-RapC-SinR quorum sensing dynamic regulatory system, the C_m^r - P_{e9} -eGFP fragment was introduced into BS168 to form strain BP03. The constitutive promoter P_{hag} was used to express *rapC* in BP03, resulting in strain BP04. The promoter Phag-*phrC* was introduced into BP04 to obtain strain BP05. Using these strains to examine the effect of cell density on the transcription efficiency of mutated promoter.

Table 1 Strains and related plasmids in this study

Names	Characteristics	Source
Strains		
<i>B. subtilis</i> 168		
BS01	BS168:: Δ aroA	lab stock
BS02	BS168:: Δ aroH	this study
BS03	BS168:: Δ trpE	this study
BS04	BS168:: Δ pabAB	this study
BS05	BS168:: Δ dhbB	this study
BS06	BS168:: Δ alsS-D	this study
BX00	BS168::P _{grac100} -sinR	this study
BX01	BS168::P _{grac100} -sinR::P _{tapA} -eGFP	this study
BX02	BS168::P _{grac100} -sinR::P _{epsA} -eGFP	this study
BX03	BS168::P _{grac100} -sinR::P _{spollA} -eGFP	this study
BX04	BS168::P _{grac100} -sinR::P _{slrR} -eGFP	this study
BX05	BS168::P _{grac100} -sinR::P _{aprE} -eGFP	this study
BX06	BS168::P _{grac100} -sinR::P _{epr} -eGFP	this study
BX07	BS168::P _{grac100} -sinR::P _{sacB} -eGFP	this study
BX08	BS168::P _{grac100} -sinR::P _{amyE} -eGFP	this study
BX09	BS168::P _{grac100} -sinR::P _{codY} -eGFP	this study
BG1	BS168::P _{grac100} -sinR::P _{e1} -eGFP	this study
BG2	BS168::P _{grac100} -sinR::P _{e2} -eGFP	this study
BG3	BS168::P _{grac100} -sinR::P _{e3} -eGFP	this study
BG4	BS168::P _{grac100} -sinR::P _{e4} -eGFP	this study
BG5	BS168::P _{grac100} -sinR::P _{e5} -eGFP	this study
BG6	BS168::P _{grac100} -sinR::P _{e6} -eGFP	this study
BG7	BS168::P _{grac100} -sinR::P _{e7} -eGFP	this study
BG8	BS168::P _{grac100} -sinR::P _{e8} -eGFP	this study
BG9	BS168::P _{grac100} -sinR::P _{e9} -eGFP	this study
BG10	BS168::P _{grac100} -sinR::P _{e10} -eGFP	this study
BG11	BS168::P _{grac100} -sinR::P _{e11} -eGFP	this study
BG12	BS168::P _{grac100} -sinR::P _{e12} -eGFP	this study
BG13	BS168::P _{grac100} -sinR::P _{e13} -eGFP	this study
BG14	BS168::P _{grac100} -sinR::P _{e14} -eGFP	this study
BG15	BS168::P _{grac100} -sinR::P _{e15} -eGFP	this study
BG16	BS168::P _{grac100} -sinR::P _{e16} -eGFP	this study
BG17	BS168::P _{grac100} -sinR::P _{e17} -eGFP	this study
BG18	BS168::P _{grac100} -sinR::P _{e18} -eGFP	this study
BG19	BS168::P _{grac100} -sinR::P _{e19} -eGFP	this study
BP00	BS168::sinR-eGFP	this study
BP01	BS168::sinR-eGFP::P _{grac100} -rapC	this study
BP02	BS168::sinR-eGFP::P _{grac100} -phrC	this study
BP03	BS168::P _{e9} -eGFP	this study
BP04	BS168::P _{e9} -eGFP::P _{hag} -rapC	this study
BP05	BS168::P _{e9} -eGFP::P _{hag} -rapC::P _{hag} -phrC	this study
BP06	BS168::P _{hag} -phrC::P _{hag} -rapC	this study
BW1	BS168::P _{hag} -rapC::P _{hag} -phrC::P _{e11} -aroA	this study
BW2	BS168::P _{hag} -rapC::P _{hag} -phrC::P _{e11} -aroA::P _{e9} -aroH	this study
BW3	BS168::P _{hag} -rapC::P _{hag} -phrC::P _{e11} -aroA::P _{e9} -aroH::P _{e9} -trpE	this study
BW4	BS168::P _{hag} -rapC::P _{hag} -phrC::P _{e11} -aroA::P _{e9} -aroH::P _{e9} -trpE::P _{e9} -dhbB	this study
BW5	BS168::P _{hag} -rapC::P _{hag} -phrC::P _{e11} -aroA::P _{e9} -aroH::P _{e9} -trpE::P _{e9} -dhbB::P _{e9} -alsA-D	this study
BW6	BS168::P _{hag} -rapC::P _{hag} -phrC::P _{e11} -aroA::P _{e9} -aroH::P _{e9} -trpE::P _{e9} -dhbB::P _{e13} -alsA-D	this study
BW7	BS168::P _{hag} -rapC::P _{hag} -phrC::P _{e11} -aroA::P _{e9} -aroH::P _{e9} -trpE::P _{e9} -dhbB::P _{e16} -alsA-D	this study
BW8	BS168::P _{hag} -rapC::P _{hag} -phrC::P _{e11} -aroA::P _{e9} -aroH::P _{e9} -trpE::P _{e9} -dhbB::P _{e17} -alsA-D	this study
BL21-eGFP	Containing eGFP	lab stock

Table 1 (continued)

Names	Characteristics	Source
plasmids		
P7C6	Pmd18-T, containing <i>lox71-zeo-lox66</i> cassette	lab stock
pHT-XCR6	Amp, C _m ^r , containing promoter P _{grac100}	lab stock
pHT-Cre	Amp, Km, <i>E. coli</i> – <i>B. subtilis</i> shuttle vector, containing cre under the control of P _{spac}	lab stock

MK-7 extraction and determination

The mutant strain was streaked onto LB plates and incubated at 37°C. A single colony was then selected and cultured overnight in LB medium with continuous shaking to ensure optimal growth conditions. The resulting seed culture was inoculated into 50 mL of fermentation medium in a 250 mL flask, with the inoculum constituting 2% of the total fermentation broth volume. The culture was grown at 37°C for 6 days. Subsequently, 2 mL of the fermentation mixture was transferred to a 5 mL brown centrifuge tube and centrifuged at 10,000 r/min for 5 min. The MK-7 present in both the precipitate and the supernatant was extracted using four volumes of extracting agent (N-hexane: isopropanol 2:1, v/v). Following a 30-minute incubation period in the dark, the upper extract was carefully collected and filtered through a 0.22 µm filter to ensure clarity. The filtered extract was then analyzed by HPLC using a 4.6 mm × 155 mm Shimadzu C-18 column. The mobile phase consisted of dichloromethane: methanol (1:9), the column temperature was maintained at 35°C, the flow rate was set to 1.0 mL/min, and the detection wavelength was 245 nm [33].

Results and discussion

Analysis of the MK-7 biosynthesis pathway in *B. subtilis*.

The MK-7 biosynthesis pathway in *B. subtilis* (Fig. 1) is organized into four distinct modules: Module I, glycerol metabolism; Module II, the shikimate (SA) pathway; Module III, the methylerythritol phosphate (MEP) pathway; and Module IV, the MK pathway [34, 35]. A detailed analysis of the MK-7 metabolic pathway has revealed the presence of multiple byproduct metabolic pathways that compete with MK-7 for essential precursor substances. For instance, For example, chorismic acid (CHA) is converted to prephenic acid by 3-deoxy-7-phosphoheptulonate synthase (AroA)/chorismate mutase (AroH) for phenylalanine (Phe) and tyrosine (Tyr) biosynthesis, or to tryptophan (Trp) via anthranilate synthase (TrpE). Additionally, para-aminobenzoate synthase (PabA/PabB) catalyzes CHA to folic acid. Phe, Tyr, and Trp feedback inhibit DAHP synthase, reducing MK-7 substrates [9]. Bifunctional isochorismate lyase/aryl carrier protein (DhbB) converts isochloroate to dihydroxybenzoate. Under high carbon metabolism or NADH, pyruvate is metabolized to hydroxybutanone by acetolactate synthase (AlsS)/acetolactate decarboxylase (AlsD), consuming carbon sources

[36]. The competition for substrates and the feedback inhibition exerted by these byproducts can significantly impact MK-7 synthesis. To address this, selection of genes involved in byproduct synthesis was undertaken to inhibit their activity, thereby redirecting precursor substances towards MK-7 synthesis.

To investigate the impact of bypass pathways on MK-7 synthesis in *Bacillus subtilis*, we conducted a systematic gene knockout study targeting key enzymes involved in competing metabolic routes. Specifically, the *aroA*, *aroH*, *trpE*, *pabAB*, *dhbB*, and *alsS-alsD* operon loci were disrupted, generating six mutant strains (BS01-BS06). These strains were fermented to evaluate their MK-7 production capabilities relative to the wild-type strain BS168.

Unexpectedly, all engineered mutant strains demonstrated significantly diminished MK-7 production relative to the wild-type strain, as illustrated in Fig. 2A. This outcome was contrary to our initial hypothesis, which anticipated a redirection of metabolic flux toward MK-7 biosynthesis upon elimination of competing pathways. Among the mutants, BS01 exhibited the most substantial decrease, with MK-7 yield reduced by 63.14% compared to the wild-type. Similarly, BS02-BS06 produced, 7.92, 11.01, 6.63, 6.75 and 5.77 mg/L of MK-7, respectively, reflecting marked reductions from the wild-type level. Notably, BS03 showed a less pronounced decline in MK-7 yield, suggesting a comparatively minor perturbation to cellular metabolism resulting from the *trpE* knockout.

Concurrently, all mutant strains demonstrated reduced biomass accumulation, as measured by optical density at 600 nm (OD₆₀₀) (Fig. 2B). After 132 h of fermentation, BS01 exhibited the most significant reduction in biomass, with an OD₆₀₀ value of 16.15 compared to 30.67 in BS168. The other mutants also showed decreased biomass levels, with BS02, BS03, BS04, BS05 and BS06 having OD₆₀₀ values of 17.81, 20.12, 25.81, 20.51, and 17.39, respectively.

These results imply that the targeted genes disruptions may have inadvertently compromised essential metabolic processes, thereby highlighting the intricate interconnectivity within the metabolic network of *Bacillus subtilis* and the need for a more nuanced approach to metabolic engineering in this organism. Dynamic metabolic engineering, using genetically encoded control systems responsive to cell density, offers a potential solution to balance growth and MK-7 synthesis. We aim to develop a dynamically controlled system that preserves the normal expression of critical genes during the

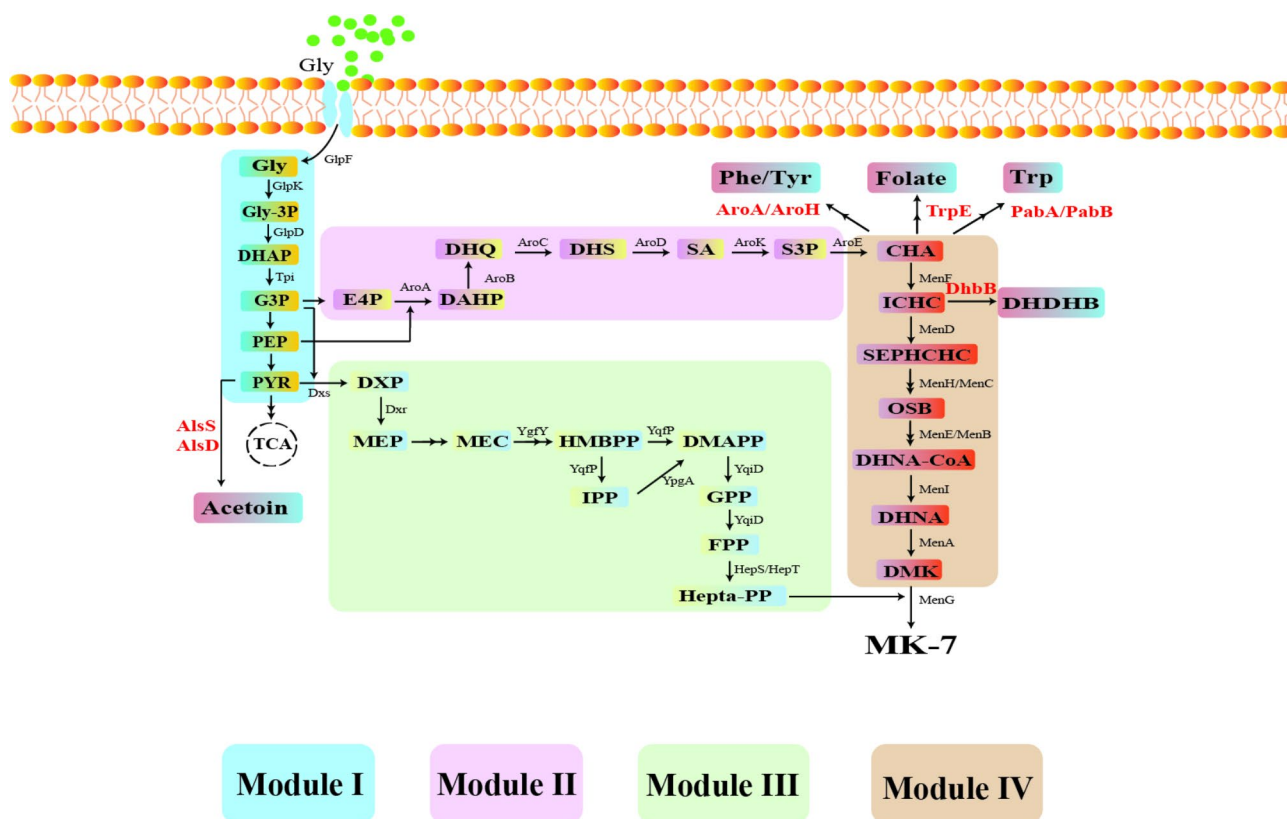


Fig. 1 Biosynthetic pathway of menaquinone-7 in *Bacillus subtilis*. Enzymes: GlpF: glycerol uptake facilitator, GlpK: glycerol kinase, GlpD: glycerol-3-phosphate dehydrogenase, Tpi: triosephosphate isomerase, Dxs: 1-deoxyxylulose-5-phosphate synthase, Dxr: 1-deoxyxylulose-5-phosphate reductoisomerase, YgfY: 4-hydroxy-3-methylbut-2-enyl diphosphate synthase, YqfP: 4-hydroxy-3-methylbut-2-enyl diphosphate reductase, YpgA: isopentenyl-diphosphate δ -isomerase, YqiD: farnesyl diphosphate synthase, AroA: 3-deoxy-7-phosphoheptulonate synthase, AroB: 3-dehydroquininate synthase, AroC: 3-dehydroquininate dehydratase, AroD: shikimate dehydrogenase, AroK: shikimate kinase, AroE: 3-phosphoshikimate-1-carboxyvinyltransferase, AroF: chorismate synthase, MenF: isochorismate synthase, MenD: 2-succinyl-5-enolpyruvyl-6-hydroxy-3-cyclohexene-1-carboxylate synthase, MenH: 2-succinyl-6-hydroxy-2,4-cyclohexadiene-1-carboxylate synthase, MenC: o-succinylbenzoate synthase, MenE: o-succinylbenzoic acid-CoA ligase, MenB: 1,4-dihydroxy-2-naphthoyl-CoA synthase, MenI: 1,4-dihydroxy-2-naphthoyl-CoA hydrolase, MenA: 1,4-dihydroxy-2-naphthoate heptaprenyltransferase, MenG: demethylmenaquinone methyltransferase, HepS/HepT: heptaprenyl diphosphate synthase component I/II. Ldh: lactate dehydrogenase, AlsS: acetolactate synthase, AlsD: acetolactate decarboxylase, AroH: chorismate mutase, TrpE: anthranilate synthase, PabB/PabA: para-aminobenzoate synthase component I/II, DhbB: bifunctional isochorismate lyase/aryl carrier protein. Abbreviations of metabolites: Gly: glycerol, Gly-3P: glycerol-3-phosphate, DAHP 3-deoxy-arabino-heptulonate 7-phosphate, G3P: glyceraldehyde-3-phosphate, PEP: phosphoenolpyruvate, PYR: pyruvate, E4P: erythrose 4-phosphate, DHQ: 3-dehydroquininate, DHS 3-dehydroshikimate, SA shikimate, S3P: shikimate 3-phosphate, CHA: chorismate, DXP: 1-deoxyxylulose-5-phosphate, MEP: methyl-erythritol-4-diphosphate, HMBPP: 1-hydroxy-2-methyl-2-butenyl 4-diphosphate, DMAPP: dimethylallyl diphosphate, IPP: isopentenyl diphosphate, GPP: geranyl diphosphate, FPP: farnesyl diphosphate, ICHA: isochorismate, SEPHCHC: 2-succinyl-5-enolpyruvyl-6-hydroxy-3-cyclohexene-1-carboxylate, OSB: 2-succinylbenzoate, DHNA-CoA: 1,4-dihydroxy-2-naphthoyl-CoA, DHNA: 1,4-dihydroxy-2-naphthoate, DMK: 2-demethylmenaquinone, MK-7: menaquinone-7, DHDHB: (2 S,3 S)-2,3-dihydro-2,3-dihydroxybenzoate, Phe: phenylalanine, Tyr: tyrosine, Trp: tryptophan

bacterial growth phase. As the culture transitions into the fermentation phase, this system will be engineered to downregulate competitive metabolic pathways, thereby redirecting metabolic resources towards enhanced MK-7 biosynthesis.

Screening and optimization of the SinR-targeted promoters

In *Bacillus subtilis*, SinR serves as a crucial transcriptional factor that binds to specific binding sites within promoter sequences to inhibit the expression of downstream genes [37]. Therefore, we propose to replace the native promoters of genes encoding enzymes involved in

byproduct synthesis with SinR-responsive promoters. By exploiting SinR's repressor activity [38], we aim to downregulate the transcription of these genes during the MK-7 fermentation phase. To further enhance SinR's regulatory efficiency, we conducted a systematic screening of SinR-targeted promoters and optimized their sequences to broaden the scope of SinR-mediated transcriptional repression.

Screening of the SinR-targeted promoters

In *Bacillus subtilis*, the SinR transcription factor engages in intricate interactions with a diverse array of proteins and regulatory factors, including TapA, EpsA, SlrR, AprE,

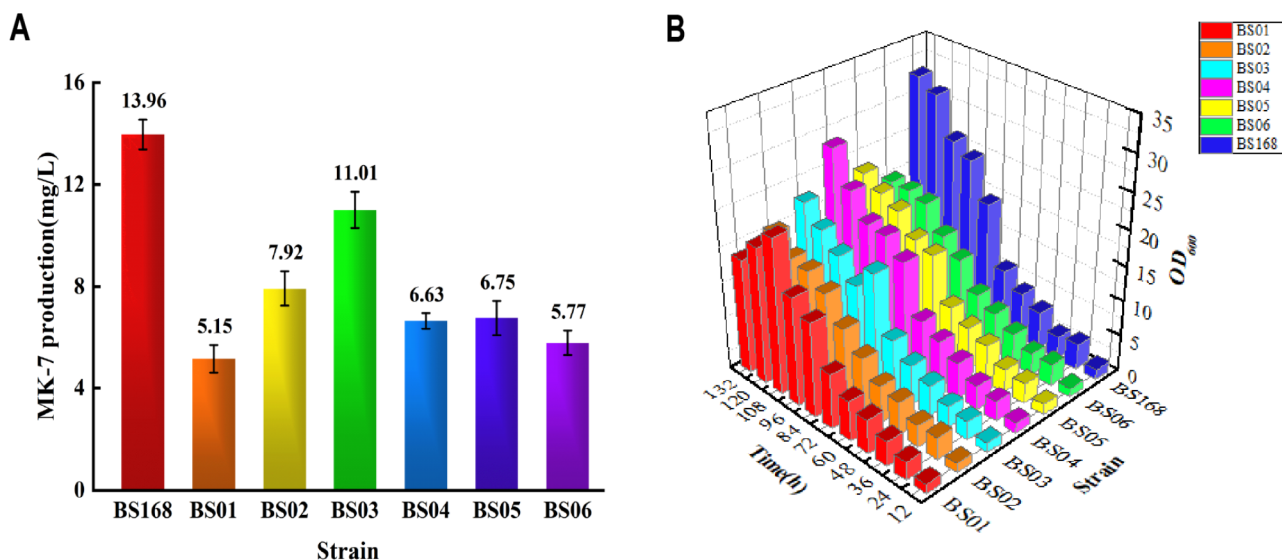


Fig. 2 Comparison of yield of menaquinone-7 (MK-7) and OD600 values for recombinant strain BS01-BS06 and original strain BS168. (A) final MK-7 yield after 132 h of BS01-BS06 and BS168 fermentation; (B) OD600 change of BS01-BS06 and BS168 during fermentation. Fig. 2A has too many reserved digits after the decimal point, which is different from the full-text number format

SpoIIA, SinI, SacB, SipW, SlrA, Epr, and CodY. These interactions orchestrate cellular processes such as protease production, natural genetic competence development, flagellar assembly, and biofilm formation [38–42]. These biological processes have the potential to alter cellular states, metabolite profiles, and nutrient availability, which in turn can modulate MK-7 synthesis by influencing the development of biofilms or spores [43].

To determine whether SinR directly binds to and regulates the promoters of genes encoding the aforementioned proteins/regulatory factors, we constructed an eGFP reporter system containing each target promoter. After inducing SinR expression with IPTG, we performed quantitative analysis of relative fluorescence intensity in bacterial cultures harboring different promoter-eGFP fusion constructs. By comparing fluorescence signals across experimental groups, we ultimately identified specific promoter that were transcriptionally repressed by SinR.

To characterize the effect of SinR concentration on promoter regulation, we engineered a tunable gene expression system in BS168. This system achieved IPTG-inducible control of *sinR* transcription under the P_{grac100} promoter, resulting in the construction of strain BX00 (using primer pairs BX00-1 to BX00-6, Fig. 3C). For systematic assessment of SinR's regulatory potency across distinct promoter architectures, we engineered nine reporter strains (BX01-BX09) each harboring a different promoter-eGFP fusion: P_{tapA} , P_{epsA} , P_{spoIIA} , P_{slrR} , P_{aprE} , P_{epr} , P_{sacB} , P_{amyE} , P_{codY} . Relative fluorescence intensity were performed to evaluate SinR-mediated repression efficiency across these promoter.

Figure 3D demonstrates the impact of SinR on promoter activities. Upon addition of 40 μM IPTG, the relative fluorescence intensities of reporter strains driven by P_{tapA} , P_{epsA} , P_{spoIIA} , P_{slrR} , P_{epr} and P_{amyE} promoters exhibited significant reductions. These results indicate that SinR exerts a repressive effect on the transcriptional output of P_{tapA} , P_{epsA} , P_{spoIIA} , P_{slrR} , P_{epr} and P_{amyE} . Notably, the inhibitory action of SinR was most pronounced for P_{tapA} , P_{epsA} , and P_{slrR} , with BX01, BX02, and BX04 showing fluorescence intensity reductions of 31.05%, 37.82%, and 23.14%, respectively. Based on these findings, P_{tapA} , P_{epsA} , and P_{slrR} were prioritized for subsequent in-depth characterization.

To characterize the concentration-dependent regulatory effects of SinR on target promoters, we conducted a dose-response analysis by inducing strains BX01, BX02, and BX04 with varying IPTG concentrations. Figure 3E shows that increasing IPTG concentrations led to a progressive decrease in relative fluorescence intensity across all three strains. Quantitative analysis revealed that SinR exhibited the most potent regulatory activity on the P_{epsA} promoter: at 60 μM IPTG, strain BX02 demonstrated a 54.09% reduction in relative fluorescence intensity compared to the IPTG-free control. This quantitative finding establishes SinR as a potent transcriptional repressor of the P_{epsA} promoter at defined concentration thresholds. Given its remarkable regulatory efficiency, the P_{epsA} promoter was prioritized for subsequent mechanistic investigations.

Optimization of the SinR-targeted promoter P_{epsA}

Structural studies revealed that SinR's N-terminal domain binds directly to a promoter motif, inducing localized

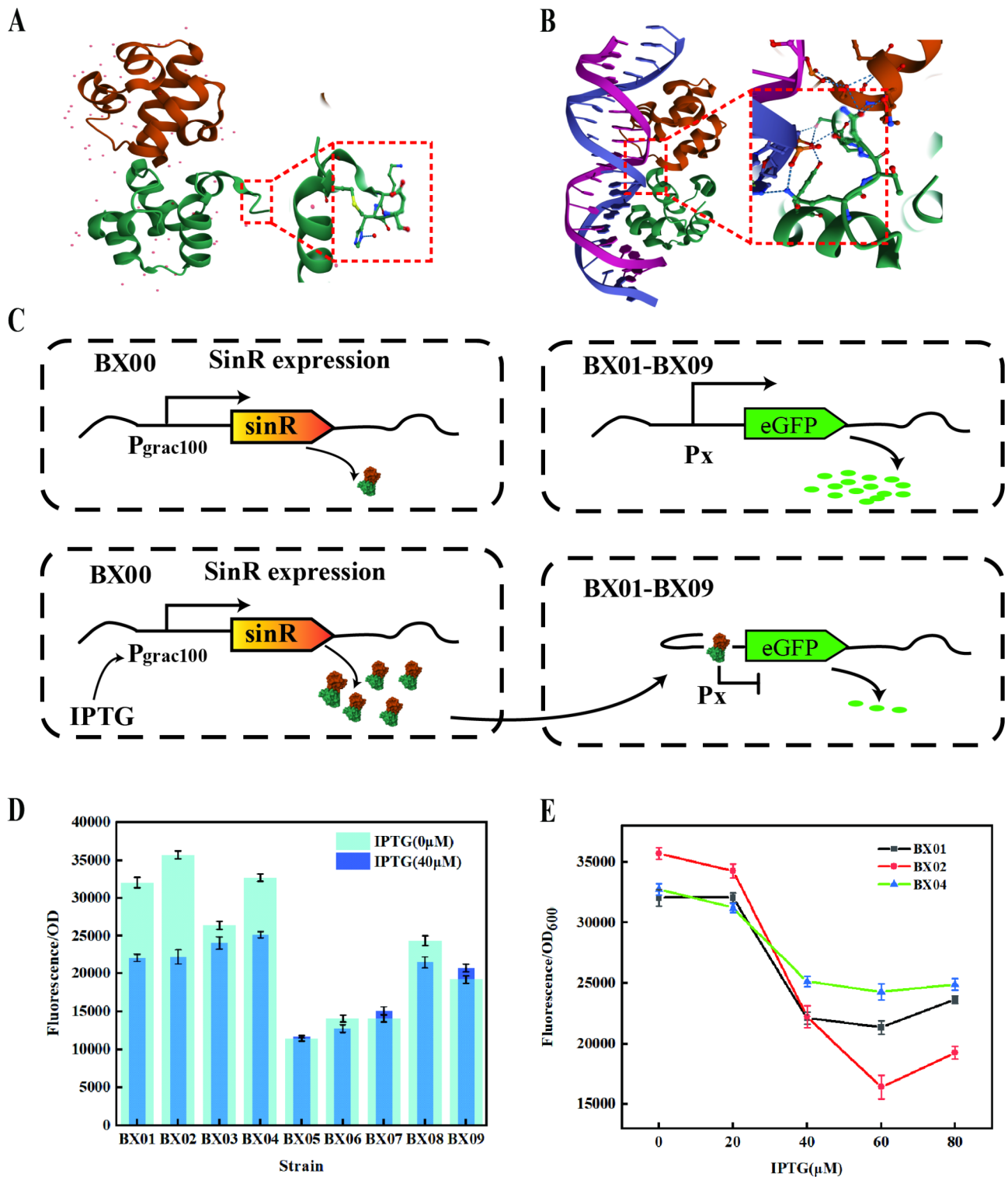


Fig. 3 Verification of the SinR Target Promoter. **(A)** SinR structure, the red dashed box shows the N-terminal domain; **(B)** simulated structure of SinR bound DNA; **(C)** the process of SinR regulation after induction by IPTG: in the absence of IPTG induction, BX00 expressed a small amount of SinR, unable to regulate eGFP expression in BX01-BX09 (two plots of the upper layer); upon the addition of IPTG, a large amount of SinR was produced, which bent the DNA in the target promoter region and inhibited the expression of eGFP (two plots of the lower layer); **(D)** before and after the addition of the IPTG, relative fluorescence intensity change of BX01-BX09 strain; **(E)** relative fluorescence intensity change of strains BX01, BX02 and BX04 with IPTG concentration

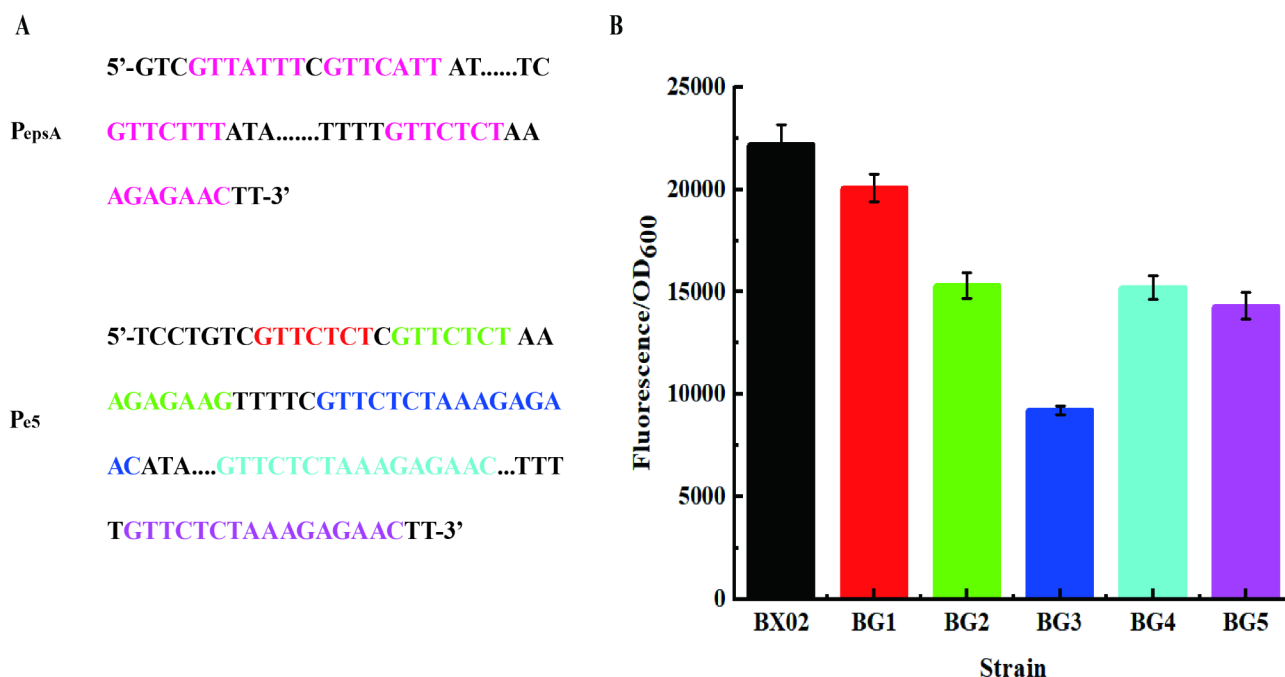


Fig. 4 Effect of the number of SinR binding sites on transcription efficiency. **A**) schematic diagram of promoter mutation; **B**) effect of different number of binding sequences on promoter transcription efficiency

DNA bending (Fig. 3A, B) [44, 45]. This aligns with the known SinR recognition sequence (-GTTCTYT-) and its high-affinity for -GTTCTCTNNAGAGAAC- reverse repeats [26, 30]. Core promoters, containing -35/-10 elements and the -16 spacer, are critical for σ factor binding and transcription initiation, making them prime targets for engineering [46].

Leveraging these insights, we implemented a rational promoter engineering strategy: (1) mutating SinR motifs in the native P_{epsA} promoter and varying the numbers of SinR recognition sites, and (2) modifying the promoter core region.

Comparative analysis revealed that the wild-type P_{epsA} promoter in *Bacillus subtilis* 168 contains SinR-binding motifs resembling the consensus sequences “GTTCTYT” or “GTTYTYT” and a inverted repeat sequences “GTTCTCTAAAGAGAAC.” To engineer promoters with enhanced SinR-mediated repression, we first mutated the original single motif to “GTTCTCT,” followed by inserting the full palindromic sequence “GTTCTCTAAAGAGAAC.” This sequential modification generated five distinct promoter variants (Fig. 4A). These engineered promoters were synthesized using primers P_{e1} to P_{e5} (Table S1), and transformed into host strains BX02 to create strains BG1-BG5. Functional screening was performed by measuring relative fluorescence intensity in bacterial cultures, identifying the optimal promoter variant that the SinR-targeted transcriptional repression. Figure 4B illustrates that the greatest decrease in fluorescence intensity was observed in BG3, with a 58.48% reduction in relative fluorescence intensity

compared to BX02. Notably, the relative fluorescence intensities of BG4 and BG5 exhibited an increase compared to BG3. Consequently, promoter P_{e3} was selected for further optimization due to its superior repressibility and distinct activity profile among the tested variants.

Initially, the promoter core region (-35 box) of P_{e3} was mutated using primer pairs listed in Table S1, generating promoters P_{e6} - P_{e11} . These were then substituted in situ for P_{e3} in strain BG3, resulting in strains BG6-BG11. To investigate the regulatory effects of SinR on the mutated promoters, SinR was induced, and the fluorescence intensity and cell density of the bacterial cultures were measured. Among all tested strains, BG9 exhibited the lowest relative fluorescence intensity. The eGFP fluorescence intensity induced by P_{e9} was reduced by 77.10% compared to that induced by P_{e3} , indicating the strongest inhibitory effect of SinR on promoter P_{e9} (Fig. 5B).

Subsequently, the -16 region of P_{e9} was optimized, yielding promoters P_{e12} - P_{e19} . These optimized promoters were introduced into BG9, generating strains BG12-BG19. Measurement of the relative fluorescence intensity of these cultures revealed that modification of the -16 region enhanced the transcriptional efficiency of all promoters (Fig. 5C). This enhancement may be attributed to two potential mechanisms. First, the extended promoter length may alleviate the bent DNA structure formed by SinR-DNA binding, thereby reducing steric hindrance to transcription. Second, alterations in the core promoter region may enhance the recruitment of RNA polymerase, leading to increased transcriptional efficiency.

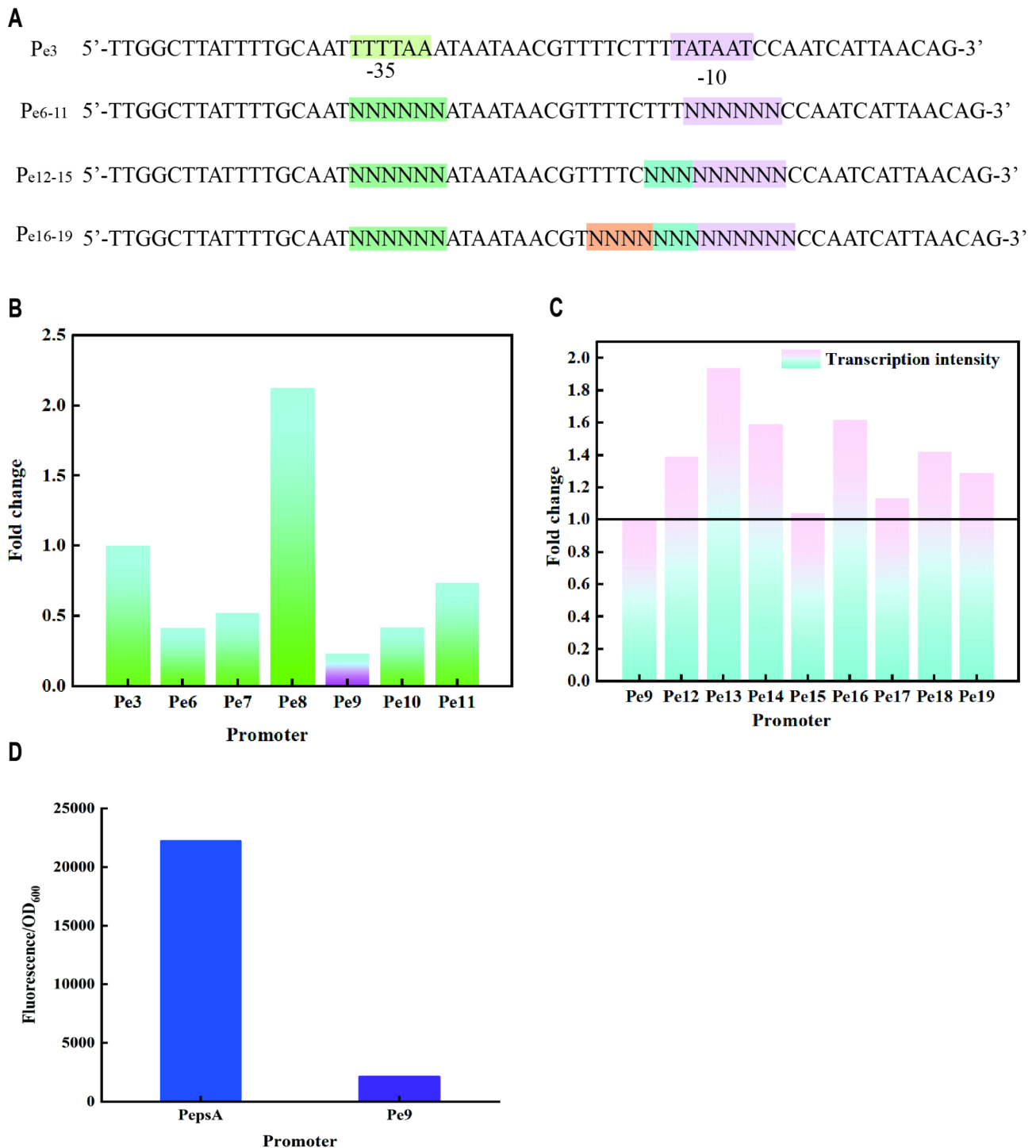


Fig. 5 Effect of the core region on the promoter transcription efficiency. **A)** schematic diagram of promoter mutation; **B)** fold change in promoter transcription efficiency after mutation in the -35 and -10 regions of P_{ε₃}; **C)** fold change in promoter transcription efficiency after mutation in the -16 region of P_{ε₉}; **D)** comparison of promoter transcription efficiency of P_{ε_{psA}} and P_{ε₉}

Construction of the PhrC-RapC-SinR QS system

RapC is known to inhibit SinR activity by ComA [27, 28], and PhrC stimulates the expression of ComA-dependent genes by repressing RapC [19]. To confirm RapC's inhibition of SinR, GFP was used to monitor SinR activity.

IPTG was added to BP01 bacterial cultures, and the relative fluorescence intensity of the cultures was measured at 4, 8, 12, and 16 h post-induction. Compared with the bacterial solution without the addition of inducer, the relative fluorescence intensity of the bacterial solution

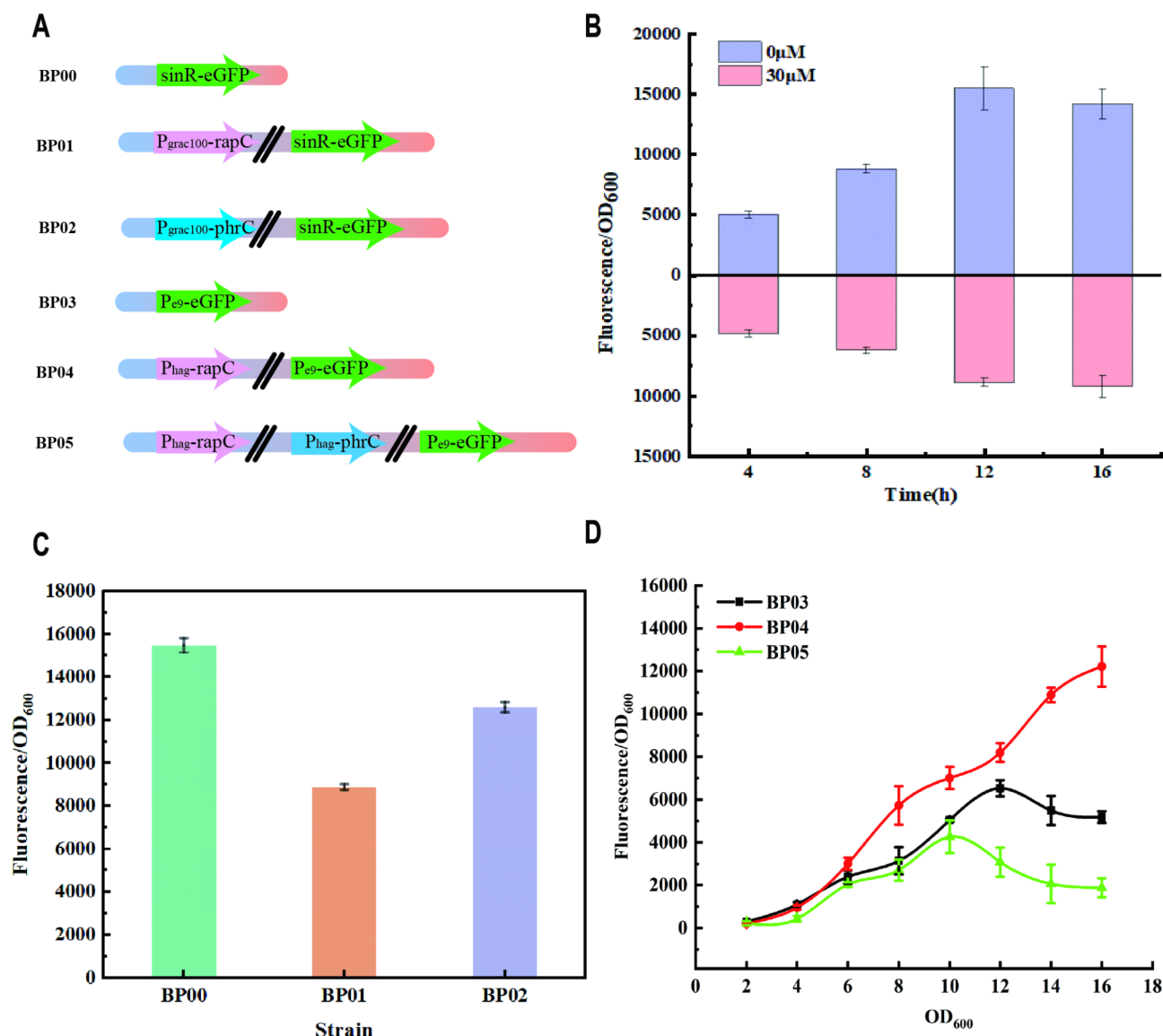


Fig. 6 Construction of the RapC-PhrC-SinR. **A**) genotype schematic representation of the strain BX00-BX05; **B**) the regulatory effect of *rapC* on *sinR*; **C**) the regulatory effect of PhrC-RapC on *sinR*; **D**) the response of the PhrC-RapC-SinR system to bacterial density

decreased significantly after the addition of IPTG. Specifically, the greatest change in relative fluorescence intensity was observed at 12 h post-IPTG induction, where it decreased to 57.37% of that in the non-IPTG-treated group (Fig. 6B). This finding demonstrates that RapC expression can suppress SinR activity.

To explore the regulatory effects of PhrC on RapC-SinR, we engineered strain BP02 by replacing the native P_{phrC} promoter in BP01 with the inducible P_{grac100} promoter. This modification allowed for controlled expression of *phrC* upon IPTG induction, enabling us to specifically interrogate its role in modulating RapC-mediated suppression of SinR. By measuring the fluorescence intensity of eGFP, a reporter protein downstream of SinR, we could quantitatively assess the impact of

PhrC-RapC interactions on SinR activity. Notably, BP02 demonstrated a 72.53% increase in eGFP fluorescence intensity compared to BP01, suggesting that PhrC expression effectively alleviates RapC-mediated repression of SinR. However, the fluorescence-to-cell density ratio only recovered to 79.10% of the baseline value observed in the absence of RapC inhibition (BP00). This partial recovery implies that, while PhrC can significantly counteract RapC's suppressive effects, full restoration of SinR activity may be contingent upon additional regulatory factors or specific physiological conditions (Fig. 6C). This partial recovery implies that, while PhrC can significantly counteract RapC's suppressive effects, it cannot fully restore SinR activity that has been inhibited by RapC.

To investigate the regulatory effects of the PhrC-RapC-SinR QS system on the engineered promoter, we constructed three bacterial strains: BP03, BP04, and BP05. In BP03, the eGFP reporter gene was inserted downstream of the P_{e9} promoter with the strongest transcriptional repression post-modification. In BP04 and BP05, expression of *rapC* and *phrC-rapC* was controlled by the constitutive promoter P_{hag} , respectively (Fig. 6A). This setup allowed us to monitor the dynamic modulation of SinR on promoter activity under QS regulation.

The results revealed distinct fluorescence patterns in BP04 and BP05. In BP04, relative fluorescence intensity increased continuously with cell density, as P_{hag} -driven RapC expression persistently repressed SinR activity, enabling unhindered eGFP expression from the P_{e9} promoter. Conversely, in BP05, relative fluorescence intensity initially rose but declined after reaching an OD₆₀₀ of 10.3. This biphasic response can be attributed to the PhrC-RapC-SinR QS system. At lower cell densities (OD₆₀₀ < 10.3), insufficient intracellular PhrC levels permitted normal P_{e9} -driven eGFP transcription, similar to BP03 and BP04. However, as cell density increased, PhrC accumulation alleviated RapC-mediated SinR suppression, restoring SinR's inhibitory effect on the promoter and subsequently reducing fluorescence intensity (Fig. 6D).

These findings collectively suggest that the PhrC-RapC-SinR QS system functions as a cell density-dependent genetic switch, capable of repressing target gene transcription in a population-responsive manner. This regulatory mechanism operates independently of metabolic pathways, exogenous inducers, or other interventions, highlighting its potential as a versatile tool for engineering cell density-responsive genetic circuits.

Dynamic fine-tuning of MK-7 synthesis in *B. subtilis* using PhrC-RapC-SinR QS system

As depicted in Fig. 7A, MK-7 synthesis exhibits a strong correlation with bacterial biomass. During the early growth phase, when OD₆₀₀ was below 4, MK-7 production was relatively slow. However, as bacterial growth progressed and the OD₆₀₀ value increased, MK-7 synthesis was significantly enhanced, indicating a growth-phase-dependent regulation of this metabolic pathway. This observation underscores the potential of dynamic regulatory systems to modulate the metabolic pathways involved in MK-7 production. Furthermore, given the crucial role of the bypass metabolic pathway in MK-7 synthesis, the knockout of genes *aroA*, *aroH*, *trpE*, *dhbB*, and *alsS-alsD* resulted in impaired bacterial growth and a subsequent reduction in MK-7 synthesis efficiency. To address this, a dynamic regulatory system, RapC-PhrC-SinR, was employed to optimize MK-7 biosynthesis,

leveraging growth-phase-dependent regulation to enhance production efficiency.

In addition to participating in the biosynthesis of prephenate, *aroA* also serves as the coding gene for DAHP synthase (AroA), which is a key enzyme catalyzing the first step reaction (conversion of PEP and E4P to DAHP) of the SA pathway [47]. Given its pivotal function, excessive repression of *aroA* expression must be avoided to prevent disruption of the SA pathway. To investigate the impact of *aroA* on MK-7 production, we replaced the native promoter of *aroA* (P_{aroA}) in situ with a series of promoters of varying strengths (P_{e1} - P_{e19}) in strain BP06. Among these, the strain harboring promoter P_{e11} , designated BW1, exhibited the highest MK-7 yield of 39.86 mg/L.

Building upon this result, we further engineered the BW1 strain by expressing *aroH*, *trpE*, *dhbB*, and *alsS-alsD* under the control of promoter P_{e9} , generating recombinant strains BW2-BW5. These strains were cultivated in 250 mL conical flasks, and their peak MK-7 yields were determined to be 52.01 mg/L, 63.93 mg/L, 72.88 mg/L, and 61.47 mg/L, respectively (Fig. 7B). These findings highlight the potential of dynamic control system as a strategy to optimize MK-7 biosynthesis by fine-tuning the expression of key genes involved in the SA pathway and related metabolic networks.

It is worth mentioning that when P_{e9} is used to express *aroH*, *trpE* and *dhbB*, the production of MK-7 was gradually increased to 72.88 mg/L. However, substituting $P_{alsS-alsD}$ with P_{e9} led to a decrease in BW5 production, with a yield of 61.47 mg/L. This phenomenon may be attributed to the overly potent inhibitory effect of promoter P_{e9} on the *alsS-alsD* operon, which results in insufficient synthesis of AlsS/AlsD. Consequently, there is an inadequate supply of hydroxybutanone for bacterial metabolism. The deficiency of hydroxybutanone not only disrupts the cellular pH balance but also exerts a profound negative impact on NADH synthesis. Since MK-7 functions as an electron transport carrier on the cell membrane of *B. subtilis*, its production levels are influenced by the NADH/NAD⁺ ratio. Efficient electron transport, which is dependent on an optimal NADH/NAD⁺ ratio, is crucial for ensuring the effective synthesis of MK-7 [48]. Therefore, regulation of the *alsS-alsD* operon necessitates the use of promoters with weaker inhibitory effects. To address this, we replaced promoter P_{e9} in strain BW5 with three promoters of varying transcription strengths: P_{e13} , P_{e16} , and P_{e17} , resulting in the generation of strains BW6-BW8 (Fig. 7C). Subsequently, we evaluated MK-7 production in these strains and discovered that strain BW7 produced the highest yield of MK-7, reaching 87.52 mg/L (Fig. 7D). This represents a 6.27-fold increase in MK-7 synthesis compared to the control strain BS168.

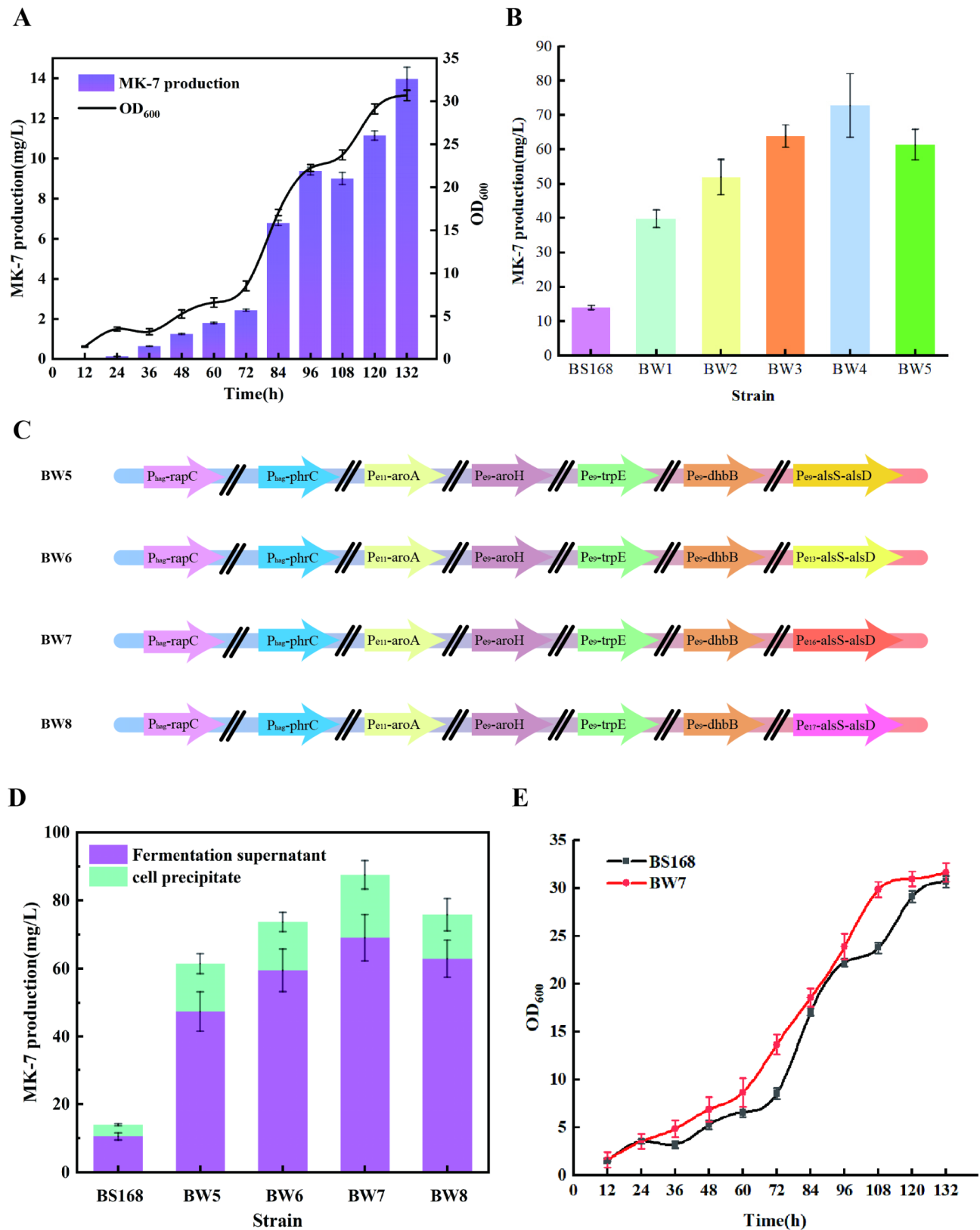


Fig. 7 Regulation of the MK-7 metabolic process by PhrC-RapC-SinR system. **A**) change of MK-7 yield and OD_{600} values over time during BS168 fermentation; **B**) MK-7 yield of strain BW1-BW5; **C**) genotype schematic representation of the strain BW5-BW8; **D**) MK-7 yield of strain BW5-BW8; **E**) comparison of OD_{600} values during fermentation of BS168 and BW7

From the growth curve presented in Fig. 7E, it is evident that the OD₆₀₀ of strain BW7 was consistently higher than that of strain BS168, suggesting that BW7 exhibited a slightly faster growth rate. Furthermore, BW7 demonstrated a prolonged stationary phase compared to BS168 after 108 h of fermentation, which may have contributed to the enhanced accumulation of MK-7. During the cell growth phase, when the OD₆₀₀ was below 10.3, the normal expression levels of genes such as *aroA* and *aroH* played a crucial role in promoting cell growth, resulting in a rapid increase in OD₆₀₀ values. As the OD₆₀₀ gradually increased, the dynamic regulatory system was activated, leading to the suppression of target gene expression. This regulatory mechanism redirected the allocation of intermediate metabolites from primarily supporting cell growth towards enhancing the MK-7 production pathway. By minimizing competition between these processes, the dynamic regulation system optimized resource utilization without impeding bacterial growth.

Conclusion

In conclusion, our study presents a significant advancement in the biotechnological production of MK-7 by introducing a novel genetic engineering strategy that combines promoter optimization with a dynamic QS regulatory system. By successfully modifying the SinR-targeted promoter P_{epsA}, we achieved a remarkable 10.50-fold change in its transcription efficiency. Furthermore, the development of the PhrC-RapC-SinR QS system represents a pioneering approach to dynamically regulate gene expression in response to cell density, providing a sophisticated mechanism to fine-tune metabolic processes.

The integration of these strategies allowed us to precisely control the expression of genes involved in byproduct synthesis pathways, thereby optimizing the allocation of cellular resources and achieving an optimal balance between cell growth and MK-7 production. The resulting 6.08-fold increase in MK-7 titer, reaching 87.52 mg/L, not only underscores the effectiveness of our approach but also highlights its potential for industrial-scale application.

The findings presented here offer a versatile platform for metabolic engineering that can be adapted to various biotechnological processes. The PhrC-RapC-SinR QS system, in particular, represents a promising tool for dynamically regulating complex metabolic networks, enabling precise control over metabolic fluxes and the optimization of product yields.

Supplementary Information

The online version contains supplementary material available at <https://doi.org/10.1186/s12934-025-02714-z>.

Supplementary Material 1

Acknowledgements

The study was supported by the National Nature Science Foundation of China (No. 32372295), Outstanding Youth Research Project in Anhui Province Universities (No. 2023AH020013), and Anhui Provincial Undergraduate Innovation and Entrepreneurship Program (No. 202310363254).

Author contributions

X.L. G.: Conceptualization, Investigation, Data curation, Formal analysis, Writing—original draft, Writing—review & editing. Y.N. L.: Conceptualization, Formal analysis, Supervision, Data curation. Y. C.: Resources, Investigation, Writing—review & editing. W. T.: investigation, Supervision. M.Y. G.: Investigation, Supervision. Y.Y. L.: Investigation, Supervision. C.C. W.: Supervision, Writing—review & editing. Y. L.: Investigation, Project administration, Resources, Supervision, Writing—original draft, Writing—review & editing, Conceptualization.

Funding

The study was supported by the National Nature Science Foundation of China (No. 32372295), Outstanding Youth Research Project in Anhui Province Universities (No. 2023AH020013), and Anhui Provincial Undergraduate Innovation and Entrepreneurship Program (No. 202310363254).

Data availability

No datasets were generated or analysed during the current study.

Declarations

Ethics approval and consent to participate

This article does not contain studies with human participants or animals performed by any of the authors.

Consent for publication

Not applicable.

Competing interests

The authors declare no competing interests.

Author details

¹College of Biological and Food Engineering, Anhui Polytechnic University, Wuhu 241000, China

²Wuhu Green Food Industry Research Institute Co., Ltd, Wuhu 238300, China

³Anhui Engineering Laboratory for Industrial Microbiology Molecular Breeding, Wuhu 241000, China

Received: 10 February 2025 / Accepted: 7 April 2025

Published online: 21 April 2025

References

- Zhang J, Zhang Y, Wang J, Xia Y, Zhang J, Chen L. Recent advances in Alzheimer's disease: mechanisms, clinical trials and new drug development strategies. *Signal Transduct Target Therapy*. 2024;9:211.
- Bloem BR, Okun MS, Klein C. Parkinson's disease. *Lancet*. 2021;397:2284–303.
- Mishima E, Wahida A, Seibt T, Conrad M. Diverse biological functions of vitamin K: from coagulation to ferroptosis. *Nat Metabolism*. 2023;5:924–32.
- Halder M, Petsophonsakul P, Akbulut AC, Pavlic A, Bohan F, Anderson E, Maresz K, Kramann R, Schurgers L. Vitamin K: double bonds beyond coagulation insights into differences between vitamin K1 and K2 in health and disease. *Int J Mol Sci* 2019;20(4):896.
- Zweers JC, Barák I, Becher D, Driessen AJM, Hecker M, Kontinen VP, Saller MJ, van Vavrová Lu JM. Towards the development of *Bacillus subtilis* as a cell factory for membrane proteins and protein complexes. *Microb Cell Fact*. 2008;7:10.
- Su Y, Liu C, Fang H, Zhang D. *Bacillus subtilis*: a universal cell factory for industry, agriculture, biomaterials and medicine. *Microb Cell Fact*. 2020;19:173.

7. Song Y, He S, Abdallah II, Jopkiewicz A, Setroikromo R, van Merkerk R, Tepper PG, Quax WJ. Engineering of multiple modules to improve amorphadiene production in *Bacillus subtilis* using CRISPR-Cas9. *J Agric Food Chem*. 2021;69:4785–94.
8. He S, Bekhof A-SMW, Popova EZ, van Merkerk R, Quax WJ. Improved taxadiene production by optimizing DXS expression and fusing short-chain prenyltransferases. *New Biotechnol*. 2024;83:66–73.
9. Yang S, Cao Y, Sun L, Li C, Lin X, Cai Z, Zhang G, Song H. Modular pathway engineering of *Bacillus subtilis* to promote de Novo biosynthesis of Menaquinone-7. *ACS Synth Biol*. 2019;8:70–81.
10. Liao C, Ayansola H, Ma Y, Ito K, Guo Y, Zhang B. Advances in enhanced Menaquinone-7 production from *Bacillus subtilis*. *Front Bioeng Biotechnol*. 2021;9:695526.
11. Zhou K, Zou R, Zhang C, Stephanopoulos G, Too HP. Optimization of amorphadiene synthesis in *Bacillus subtilis* via transcriptional, translational, and media modulation. *Biotechnol Bioeng*. 2013;110:2556–61.
12. Yang S, Wang Y, Cai Z, Zhang G, Song H. Metabolic engineering of *Bacillus subtilis* for high-titer production of menaquinone-7. *AIChE J*. 2019;66(1):e16754.
13. Tan SZ, Prather KLJ. Dynamic pathway regulation: recent advances and methods of construction. *Curr Opin Chem Biol*. 2017;41:28–35.
14. Eickhoff MJ, Bassler BL. SnapShot: bacterial quorum sensing. *Cell*. 2018;174:1328–e13281321.
15. Pappenfort K, Bassler BL. Quorum sensing signal–response systems in Gram-negative bacteria. *Nat Rev Microbiol*. 2016;14:576–88.
16. Yi L, Dong X, Grenier D, Wang K, Wang Y. Research progress of bacterial quorum sensing receptors: classification, structure, function and characteristics. *Sci Total Environ*. 2021;763:143031.
17. Liu Y, Liu L, Li J, Du G, Chen J. Synthetic biology toolbox and chassis development in *Bacillus subtilis*. *Trends Biotechnol*. 2019;37:548–62.
18. Yang X, Liu J, Zhang J, Shen Y, Qi Q, Bao X, Hou J. Quorum sensing-mediated protein degradation for dynamic metabolic pathway control in *Saccharomyces cerevisiae*. *Metab Eng*. 2021;64:85–94.
19. Auchtung Jennifer M, Lee Catherine A, Grossman Alan D. Modulation of the ComA-Dependent quorum response in *Bacillus subtilis* by multiple Rap proteins and Phr peptides. *J Bacteriol*. 2006;188:5273–85.
20. Auchtung JM, Lee CA, Grossman AD. Modulation of the ComA-Dependent quorum response in *Bacillus subtilis* by multiple Rap proteins and Phr peptides. *J bacteriol*. 2006;188(14):5273–85.
21. Pottathil M, Lazazzera BA. The extracellular Phr peptide–Rap phosphatase signaling circuit of *Bacillus subtilis*. *Front Biosci*. 2003;8(4):32–45.
22. Liang Z, Qiao JQ, Li PP, Zhang LL, Qiao ZX, Lin L, Yu CJ, Yang Y, Zubair M, Gu Q, et al. A novel Rap-Phr system in *Bacillus velezensis* NAU-B3 regulates surfactin production and sporulation via interaction with coma. *Appl Microbiol Biotechnol*. 2020;104:10059–74.
23. Parashar V, Konkol MA, Kearns DB, Neiditch MB. A plasmid-encoded phosphatase regulates *Bacillus subtilis* biofilm architecture, sporulation, and genetic competence. *J Bacteriol*. 2013;195:2437–48.
24. Zhao L, Liu Q, Xu FH, Liu H, Zhang J, Liu F, Wang G. Identification and analysis of Rap–Phr system in *Bacillus cereus* 0–9. *FEMS Microbiol Lett*. 2022;369:fnac026.
25. Hu L-x, Zhao M, Hu W-s, Zhou M-j, Huang J-b, Huang X-l, Gao X-l, Luo Y-n, Li C, Liu K, et al. Poly- γ -Glutamic acid production by engineering a DegU Quorum-Sensing circuit in *Bacillus subtilis*. *ACS Synth Biol*. 2022;11:4156–70.
26. Newman JA, Rodrigues C, Lewis RJ. Molecular basis of the activity of SinR protein, the master regulator of biofilm formation in *Bacillus subtilis***. *J Biol Chem*. 2013;288:10766–78.
27. She Q, Hunter E, Qin Y, Nicolau S, Zalis Eliza A, Wang H, Chen Y, Chai Y. Negative interplay between biofilm formation and competence in the environmental strains of *Bacillus subtilis*. *mSystems*. 2020;5. <https://doi.org/10.1128/mSystems.00539-00520>.
28. Core L, Perego M. TPR-mediated interaction of RapC with coma inhibits response regulator-DNA binding for competence development in *Bacillus subtilis*. *Mol Microbiol*. 2003;49:1509–22.
29. Wu J, Li W, Zhao S-g, Qian S-h, Wang Z, Zhou M-j, Hu W-s, Wang J, Hu L-x, Liu Y. Xue Z-l: Site-directed mutagenesis of the quorum-sensing transcriptional regulator SinR affects the biosynthesis of menaquinone in *Bacillus subtilis*. *Microb Cell Fact*. 2021;20:113.
30. Colledge VL, Fogg MJ, Levdivkov VM, Leech A, Dodson EJ, Wilkinson AJ. Structure and organisation of SinR, the master regulator of biofilm formation in *Bacillus subtilis*. *J Mol Biol*. 2011;411:597–613.
31. Wilking JN, Ziburdaev V, De Volder M, Losick R, Brenner MP, Weitz DA. Liquid transport facilitated by channels in *Bacillus subtilis* biofilms. *Proc Natl Acad Sci*. 2013;110(3):848–52.
32. Chu PTB, Phan TTP, Nguyen TTT, Truong TTT, Schumann W, Nguyen HD. Potent IPTG-inducible integrative expression vectors for production of Recombinant proteins in *Bacillus subtilis*. *World J Microbiol Biotechnol*. 2023;39:143.
33. Huang X, Gao X, Huang J, Luo Y, Tao W, Guo M, Liu Y, Wu J, Chen Y, Liu Y. Study on the effects of BdhA knockout on coproduction of menaquinone-7 and nattokinase by *Bacillus subtilis* based on RNA-Seq analysis. *Process Biochem*. 2024;144:45–53.
34. Ma Y, McClure DD, Somerville MV, Proschogo NW, Dehghani F, Kavanagh JM, Coleman NV. Metabolic engineering of the MEP pathway in *Bacillus subtilis* for increased biosynthesis of Menaquinone-7. *ACS Synth Biol*. 2019;8:1620–30.
35. Cui S, Lv X, Wu Y, Li J, Du G, Ledesma-Amaro R, Liu L. Engineering a bifunctional Phr60-Rap60-Spo0A Quorum-Sensing molecular switch for dynamic Fine-Tuning of Menaquinone-7 synthesis in *Bacillus subtilis*. *ACS Synth Biol*. 2019;8:1826–37.
36. Renna MC, Najimudin N, Winik LR, Zahler SA. Regulation of the *Bacillus subtilis* *AlsS*, *alsD*, and *AlsR* genes involved in post-exponential-phase production of acetoin. *J Bacteriol*. 1993;175:3863–75.
37. Newman JA, Rodrigues C, Lewis RJ. Molecular basis of the activity of SinR protein, the master regulator of biofilm formation in *Bacillus subtilis*. *J Biol Chem*. 2013;288:10766–78.
38. Mandic-Mulec I, Gaur N, Bai U, Smith I. Sin, a stage-specific repressor of cellular differentiation. *J Bacteriol*. 1992;174:3561–9.
39. Mandic-Mulec I, Doukhan L, Smith, IJ. The *Bacillus subtilis* SinR protein is a repressor of the key sporulation gene spo0A. *J bacteriol*. 1995;177(16):4619–27.
40. Kodgire P, Dixit M, Rao KK. ScoC and SinR negatively regulate *Epr* by corepression in *Bacillus subtilis*. *J Bacteriol*. 2006;188:6425–8.
41. Girinathan BP, Ou J, Dupuy B, Govind R. Pleiotropic roles of Clostridium difficile sin locus. *PLoS Pathogens*. 2018;14(3):e1006940.
42. Olmos J, de Anda R, Ferrari E, Bolivar F, Valle F. Effects of the SinR and degU32 (Hy) mutations on the regulation of the *AprE* gene in *Bacillus subtilis*. *Mol Gen Genet MGG*. 1997;253:562–7.
43. Yi Y, Chen M, Yang H, Zong X, Coldea TE, Zhao H. New insights into the role of cellular States, cell-secreted metabolites, and essential nutrients in biofilm formation and menaquinone-7 biosynthesis in *Bacillus subtilis* Natto. *Food Res Int*. 2025;206:116052.
44. Newman JA, Rodrigues C, Lewis RJ. Molecular basis of the activity of SinR protein, the master regulator of biofilm formation in *Bacillus subtilis* *supx2666*. *J Biol Chem*. 2013;288:10766–78.
45. Milton ME, Cavanagh J. The biofilm regulatory network from *Bacillus subtilis*: A Structure-Function analysis. *J Mol Biol*. 2023;435:167923.
46. Zhou C, Ye B, Cheng S, Zhao L, Liu Y, Jiang J, Yan X. Promoter engineering enables overproduction of foreign proteins from a single copy expression cassette in *Bacillus subtilis*. *Microb Cell Fact*. 2019;18:111.
47. Liu D-F, Ai G-M, Zheng Q-X, Liu C, Jiang C-Y, Liu L-X, Zhang B, Liu Y-M, Yang C, Liu S-J. Metabolic flux responses to genetic modification for Shikimic acid production by *Bacillus subtilis* strains. *Microb Cell Fact*. 2014;13:40.
48. Ding X, Zheng Z, Zhao G, Wang L, Wang H, Yang Q, Zhang M, Li L, Wang P. Bottom-up synthetic biology approach for improving the efficiency of menaquinone-7 synthesis in *Bacillus subtilis*. *Microb Cell Fact*. 2022;21:101.

Publisher's note

Springer Nature remains neutral with regard to jurisdictional claims in published maps and institutional affiliations.